

Superconducting single photon detectors made by local oxidation with an atomic force microscope

C. Delacour, J. Claudon, J.-Ph. Poizat, B. Pannetier, and V. Bouchiat^{a)}
Institut Néel, CNRS-Grenoble, 38042 Grenoble, France

R. Espiau de Lamaestre
CEA/Leti-MINATEC, 38042 Grenoble, France

J.-C. Villegier
CEA-G/DRFMC-SPSMS, 38042 Grenoble, France

M. Tarkhov, A. Korneev, B. Voronov, and G. Gol'tsman
Moscow State Pedagogical University, Moscow 119435, Russia

(Received 13 March 2007; accepted 13 April 2007; published online 9 May 2007)

The authors present a fabrication technique of superconducting single photon detectors made by local oxidation of niobium nitride ultrathin films. Narrow superconducting meander lines are obtained by direct writing of insulating niobium oxynitride lines through the films using voltage-biased tip of an atomic force microscope. Due to the 30 nm resolution of the lithographic technique, the filling factor of the meander line can be made substantially higher than detector of similar geometry made by electron beam lithography, thus leading to increased quantum efficiency. Single photon detection regime of these devices is demonstrated at 4.2 K. © 2007 American Institute of Physics. [DOI: 10.1063/1.2738195]

Superconducting single photon detectors¹ (SSPD) are today's most promising devices for high-speed single photon detection. Indeed they have shown lower jitter,² lower dark counts and higher bandwidth³ compared to semiconducting detectors (avalanche photodiodes). Furthermore, their good sensitivity in the near infrared makes them very useful to be used as imagers of defects in very large scale integrated circuits⁴ or as single photon detectors in quantum cryptography setups.⁵ Their detection principle is based on the conversion of the incident photon into a cascade of quasiparticles that induces a "hot spot" (i.e., a normal state region⁶) in a portion of a nanowire. With the normal state sheet resistance of such a thin film being relatively high ($\sim 350 \Omega/\text{square}$), this transient and very local resistive state generates a sub-nanosecond voltage pulse across the device which can be detected as individual single photon events.¹ Superconducting wires having a nanometer-sized cross section have proven to be necessary to let the low energy infrared photon creates a detectable hot spot. Moreover, the denser the meander line is made, the better the photonic cross section. Therefore, a large filling factor for the nanowire increases the detector quantum efficiency. Both requirements (narrow lines and high density) are highly demanding in terms of lithography. State-of-the-art resolution using electron beam lithography is usually limited by proximity effect.⁷ In this letter, we present an alternative technology allowing fabrication of ultradense superconducting meander lines. These are obtained by direct oxidation of a niobium nitride (NbN) ultrathin films using the voltage-biased tip of an atomic force microscope (AFM). This technique⁸ was pioneered in the early 1990s on silicon substrates⁹ and rapidly extended to the controlled design of quantum devices by direct writing of sub-10-nm insulating oxide lines.¹⁰ Since then many applications have been shown, including templates for molecular wires.¹¹

Metal-based quantum devices using metallic ultrathin films such as quantum point contacts,¹² single electron transistors,¹³ and magnetite constrictions¹⁴ useful for spintronics have been obtained. More recently, its use has been extended to superconducting quantum devices.¹⁵ In this letter, we follow that latter application and show the use of this oxidation technique to fabricate, in a single step, superconducting meander lines, without the use of resist or subsequent etching step. We show that the gap between superconducting strips obtained by this technique can be made significantly smaller to what is currently obtained using conventional electron beam lithography.

We start from NbN film which has been sputtered on *R*-plane sapphire using a Nb target operated in argon/nitrogen plasma.¹⁶ The total film thickness measured with an AFM is 8 nm from which we have to remove a dead layer of 2 nm consisting of native oxide. Using standard UV lithography, plasma etching, and metal deposition steps, a squared NbN pixel of $20 \times 20 \mu\text{m}^2$ active area is patterned and connected to a 100-nm-thick gold coplanar waveguide. Local oxidation of the film with the AFM operated using tapping mode¹⁷ is usually performed as the last fabrication stage. We use commercially available metal-covered tips (Pt or Pt-Ir) that is scanned over the surface at speeds around $0.1 \mu\text{m/s}$ and biased with a 10 kHz square signal of amplitude typically 15 V peak to peak. The amplitude set point during lithography is reduced to about 20% of the free amplitude and the relative humidity is kept at 50%. This gives a 12-nm-thick oxide protrusion which presents 30–70 nm full width at half maximum. This latter value depends on the tip sharpness (see Fig. 1 inset). The total oxide height (including the buried oxide) (18 nm) is consistent with the creation of a niobium oxynitride NbN_xO_y phase¹⁸ with high oxygen content that confers insulating properties.¹⁹ The superconducting meander line is then fabricated using a set of interdigitated oxide lines (see Fig. 1). The measured device is a 270-nm-

^{a)}Electronic mail: vincent.bouchiat@grenoble.cnrs.fr

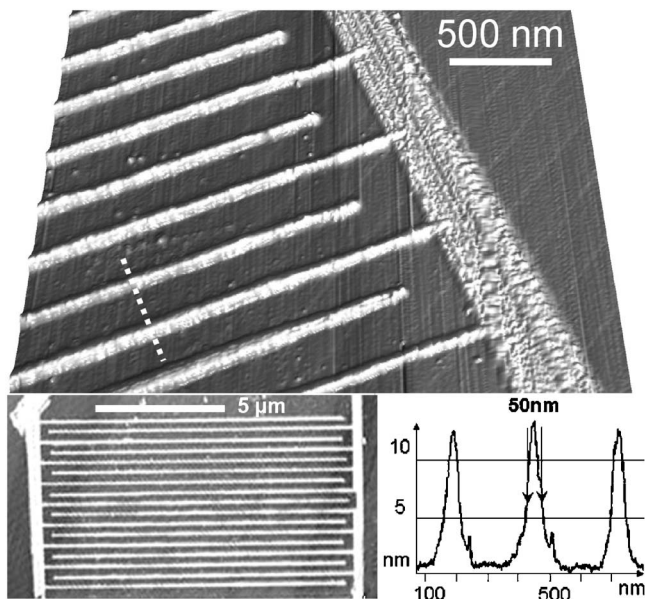


FIG. 1. (Top) AFM micrograph of NbN meander line realized by local anodization in the regime of full oxidation of a 6-nm-thick film. The brightest regions are the patterned oxide protrusions. The stripes visible on the top right of the image are 0.3 nm high atomic steps, replicated from the underlying sapphire substrate. (Bottom right) Line profile of series oxide protrusions showing a 0.25 aspect ratio. (Bottom left) General AFM micrograph of a typical sample showing the interdigitated pattern of oxide lines.

wide meander strip line, with a 320 nm pitch which leads to a developed length of 44 μm . The filling factor of the superconducting meander line can be increased up to 80% which is significantly higher to what is currently done using electron beam lithography (EBL) (typically 50%–60%, depending on the resolution achieved). Several additional advantages are provided by the oxidation technique: the regularity and surface roughness of the AFM-made superconducting lines are substantially better than what is routinely achieved by the alternative technology based on plasma etching.²⁰ Furthermore the nanowire sides are embedded in the niobium oxynitride, thus reducing aging due to further oxidation.

The detector is then placed in a liquid helium cryostat. Direct current (dc) characterization is done using RC low pass filtered lines while photon counting measurements are done using a setup similar as described in Ref. 1. Three different optical sources of different powers and wavelengths are used: a 400 nm blue light emitting diode (LED) of 3.25 mW nominal power, an 850 nm 20 ps pulse laser with a repetition rate of 100 kHz, and a 660 nm red LED.

The SSPD measured here showed a serial resistance of 36 k Ω in the normal state and a superconducting critical temperature of 9.5 K. The dc voltage source I - V curve (Fig. 2) exhibits a superconducting branch of 45 μA followed by the characteristic hot-spot plateau²¹ that develops over 100 mV before switching toward a linear branch corresponding to the normal resistance of several meander arms (7.7 k Ω). The associated critical current density is 3.5 MA/cm². Little hysteretical bumps along the hot-spot plateau are attributed to motion of free vortices (depinning) that are typical features encountered in such nanowires.^{6,21} In Fig. 2 inset is shown a time-resolved voltage pulse for the same device measured using high-speed measurement. The pulse amplitude is 100 μV (before the 75 dB amplification) and the pulse width is 2.5 ns. The overall lineshape and sub-

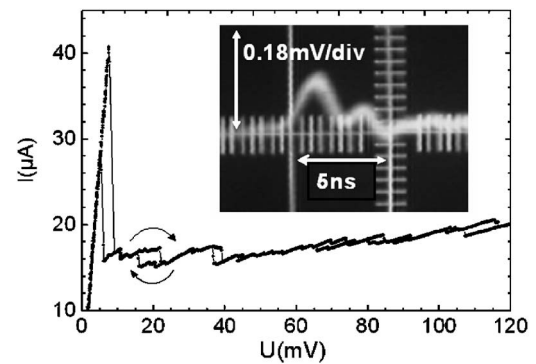


FIG. 2. Low frequency voltage-biased $I(V)$ characteristics of a typical AFM-made SSPD device measured at 4.2 K. The hot-spot plateau is at 16 μA , one third of the value of the critical current. Inset: Oscilloscope time trace of a single count event, measured in the same condition with high frequency lines (the 75 dB amplification of the rf has been subtracted).

sequent backlash is due to amplifier artifacts. Figure 3 depicts the average number of these voltage pulses measured per unit time as a function of the current bias of the detector. Note that in the following figures, the bias current is normalized by the maximum superconducting current I_c , measured before switching to the resistive state. It is expected to be very close to the critical current I_c . These measurements are repeated in darkness (squares on Fig. 3) and for constant photonic irradiation using the three different sources. All four curves roughly follow an exponential dependence with the current bias consistent to what was observed in typical SSPDs.²² The dark counts which are about 20 Hz/ μA is found to be similar to what is found in e-beam made SSPDs.³ However these dark counts most probably comes from intrinsic noise from the device and not from thermal background radiation. Figure 4 depicts the count rate dependence as a function of the average number of photons incident on the detector measured for different source wavelengths (top) and for different SSPD current biases (bottom). However, the slope of the curve depicting the number of counts versus optical source attenuation depends critically on these wavelengths. All sources are heavily attenuated to be close to the single photon regime.²⁴ A clear difference of behavior is ob-

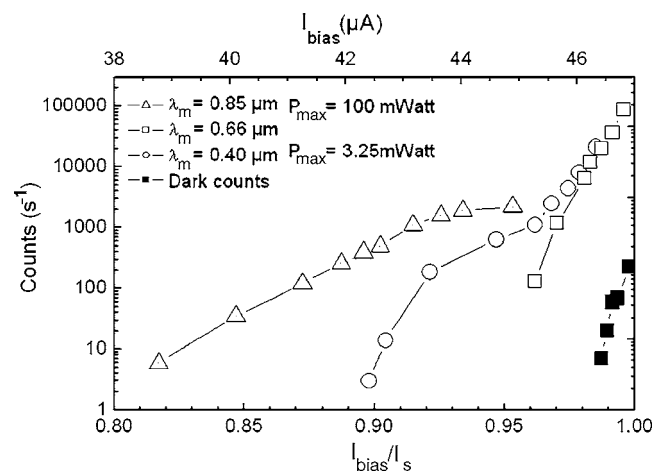


FIG. 3. Counting rates vs the bias current on an AFM-made SSPD measured at 4 K, for different photon sources as a function of the normalized bias current. (From left to right) Irradiation sources are IR laser (two-photon response), blue LED, and red LED (single-photon response). (On far right) Dark counts for the same measuring conditions.

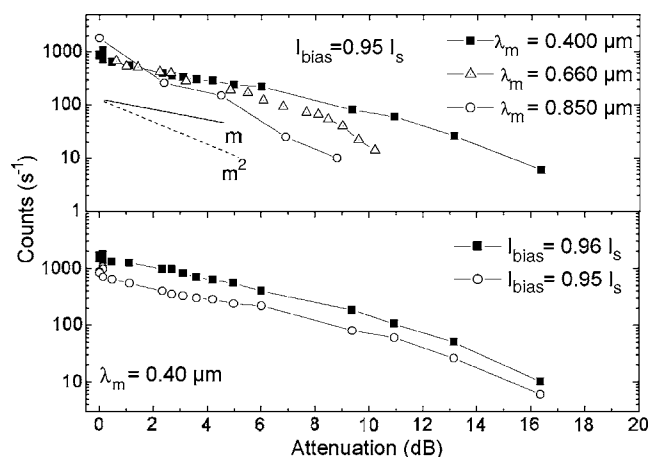


FIG. 4. (Top) Detector counting rates as a function of the sources attenuation for blue, red, and infrared irradiation and (bottom) at two different bias currents for blue irradiation.

tained depending on the source wavelength. Under blue and red irradiations, the slope of the count rates versus source attenuation plotted in log-log scale is roughly equal to one, showing a clear signature¹ of a single photon response. On the other hand, under irradiation with the IR source, one observes a roughly doubled slope which is consistent with a two photon response. When biasing the device close to the critical current (Fig. 4, bottom), one can check that this slope corresponding to the single photon regime is independent on the bias current.²³ The single photon response is preserved in finite current biasing region.

As a conclusion, we have presented fabrication and measurement of highly dense SSPDs involving fabrication using oxidation under an atomic force microscope. Single photon response is demonstrated under blue and red irradiations.

The authors thank J.-P. Maneval for stimulating discussions. This work has been partly supported by ACI Nanoscience from French Ministry of Research, D.G.A., by Grant No. 02.445.11.7434 of Russian Ministry of Education and Science, and by the European Commission under project "SINPHONIA," Contract No. NMP4-CT-2005-16433.

¹G. N. Gol'tsman, O. Okunev, G. Chulkova, A. Lipatov, A. Semenov, K. Smirnov, B. Voronov, A. Dzardanov, C. Williams, and R. Sobolewski, Appl. Phys. Lett. **79**, 705 (2001).

²R. H. Hadfield, M. J. Stevens, S. S. Gruber, A. J. Miller, R. E. Schwall,

R. P. Mirin, and S. W. Nam, Opt. Express **13**, 10846 (2005).

³A. Korneev, P. Kouminov, V. Matvienko, G. Chulkova, K. Smirnov, B. Voronov, G. N. Gol'tsman, M. Currie, W. Lo, K. Wilsher, J. Zhang, W. Sysz, A. Pearlman, A. Verevkin, and Roman Sobolewski, Appl. Phys. Lett. **84**, 5338 (2004).

⁴J. Zhang, N. Boiadjeva, G. Chulkova, H. Deslandes, G. N. Gol'tsman, A. Korneev, P. Kouminov, M. Leibowitz, W. Lo, R. Malinsky, O. Okunev, A. Pearlman, W. Sysz, K. Smirnov, C. Tsao, A. Verevkin, B. Voronov, K. Wilsher, and R. Sobolewski, Electron. Lett. **39**, 1086 (2003).

⁵R. H. Hadfield, J. L. Habif, J. Schlafer, R. E. Schwall, and S. W. Nam, Appl. Phys. Lett. **89**, 241129 (2006); W. Sysz, M. WJgrzecki, J. Bar, P. Grabiec, M. Górska, V. Zwiller, C. Latta, P. Bohi, I. Milostnaya, O. Minaeva, A. Antipov, O. Okunev, A. Korneev, K. Smirnov, B. Voronov, N. Kaurova, G. Gol'tsman, A. Pearlman, A. Cross, I. Komissarov, A. Verevkin, and R. Sobolewski, *ibid.* **88**, 261113 (2006).

⁶W. J. Skocpol, M. R. Beasley, and M. Tinkham, J. Low Temp. Phys. **16**, 145 (1974).

⁷T. H. P. Chang, J. Vac. Sci. Technol. **12**, 1271 (1975).

⁸For a recent review see R. Garcia, R. V. Martinez, and J. Martinez, Chem. Soc. Rev. **35**, 29 (2006).

⁹J. A. Dagata, J. Schneir, H. H. Harary, C. J. Evans, M. T. Postek, and J. Bennett, Appl. Phys. Lett. **56**, 2001 (1990).

¹⁰E. S. Snow and P. M. Campbell, Science **270**, 1639 (1995).

¹¹R. Garcia, M. Tello, J. F. Moulin, and F. Biscarini, Nano Lett. **4**, 1115 (2004).

¹²E. S. Snow, D. Park, and P. M. Campbell, Appl. Phys. Lett. **69**, 269 (1996).

¹³K. Matsumoto, M. Ishii, K. Segawa, Y. Oka, B. J. Vartanian, and J. S. Harris, Appl. Phys. Lett. **68**, 34 (1996).

¹⁴L. Pellegrino, E. Bellingeri, A. S. Siri, and D. Marré, Appl. Phys. Lett. **87**, 064102 (2005).

¹⁵V. Bouchiat, M. Faucher, C. Thirion, W. Wernsdorfer, T. Fournier, and B. Pannetier, Appl. Phys. Lett. **79**, 123 (2001).

¹⁶G. Gol'tsman, K. Smirnov, P. Kouminov, B. Voronov, N. Kaurova, V. Drakinsky, J. Zhang, A. Verevkin, and R. Sobolewski, IEEE Trans. Appl. Supercond. **13**, 192–195 (2003).

¹⁷F. Perez-Murano, G. Abadal, N. Barniol, X. Aymerich, J. Servat, P. Gorostiza, and F. Sanz, J. Appl. Phys. **78**, 6797 (1995).

¹⁸V. Schwartz and S. T. Oyama, Chem. Mater. **9**, 3052 (1997).

¹⁹V. E. Shaternik, G. V. Kurdyumov, and M. A. Belogolovskii, Low Temp. Phys. **29**, 993 (2003).

²⁰S. Cherednichenko, P. Yagoubov, K. Il'in, G. Gol'tsman, and E. Gershenzon, Proceedings of the 8th International Symposium On Space Terahertz Technology, Boston, MA, 1997 (unpublished), p. 245.

²¹W. J. Skocpol, M. R. Beasley, and M. Tinkham, J. Appl. Phys. **45**, 4054 (1974).

²²R. Sobolewski, Y. Xu, X. Zheng, C. Williams, K. Zhang, A. Verevkin, G. Chulkova, A. Korneev, A. Lipatov, O. Okunev, K. Smirnov, and G. N. Gol'tsman, IEICE Trans. Electron. **E85**, 797 (2002).

²³A. Engel, A. D. Semenov, H.-W. Hübers, K. Il'in, and M. Siegel, Physica C **444**, 12 (2006).

²⁴Note that the blue LED although being a continuous source is sufficiently attenuated so that the SSPD returns to equilibrium state in the average time separating two photons.